Multiple Growth Episodes or Prolonged Formation of Diamonds? Inferences from Infrared Absorption Data

M. Palot, D. G. Pearson, T. Stachel, J. W. Harris, G. P. Bulanova, and I. Chinn

Abstract

The infrared characteristics of 21 sulphide inclusion-bearing diamonds from Finsch Mine, 1 sulphide inclusion-bearing diamond from Udachnaya and 18 silicate inclusion-bearing diamonds from Premier were examined and modelled to investigate the complexity of diamond genesis. Internal heterogeneities in N-abundance and aggregation state within individual diamonds at Finsch range from 5 to 336 at.ppm and 2–60 % of B-defects, respectively. The Udachnaya diamond 3648 displays a steep decrease from the core to the rim of N-abundance from 482 to 10 at.ppm. Nitrogen aggregation state describes the same trend with value of 86 %B in the core down to 14 %B in the rim. Internal variations in N-abundance and aggregation state within diamonds from Premier are 93–654 at.ppm and of 7–62 %B, respectively. These variations reflect more likely multiple growth episodes of diamond at distinct ages rather than steady changes in temperature conditions during prolonged diamond growth. Modelling of infrared characteristics indicates that some diamonds have experienced distinct growth episodes over extended time periods with estimates up to 2,387 ± 931 Ma. There are implications for dating studies, indicating that isochron ages may be flawed as there appears to be no single formation age for a single diamond. N-abundance and aggregation state mapping by FTIR provide the opportunity to constrain diamond growth history for selecting diamonds for dating.

Keywords

Diamond • Infrared spectroscopy • Cathodoluminescence • Diamond genesis

Introduction

Diamonds are unique samples for studying the secular evolution of the lithosphere and the asthenosphere (e.g. Shirey et al. 2002; Stachel et al. 2005). Inclusions encapsulated in diamonds provide evidence for conditions of diamond growth and represent the most reliable technique of dating diamonds. Dating of silicate inclusions requires generally multiple inclusion composites from individual to several diamonds (e.g. Richardson et al. 1984, 1990). Sulphide inclusions and Re–Os isotopes enhance the possibility of dating individual (e.g. Pearson et al. 1998; Pearson and

M. Palot (✉) · D. G. Pearson · T. Stachel
Department of Earth and Atmospheric Sciences, University of Alberta, Edmonton, Canada
e-mail: palot@ualberta.ca

J. W. Harris
School of Geographical and Earth Sciences, University of Glasgow, Glasgow, UK

G. P. Bulanova
School of Earth Sciences, University of Bristol, Bristol, UK

I. Chinn
De Beers Geoscience Centre, South Africa

D. G. Pearson et al. (eds.), *Proceedings of 10th International Kimberlite Conference*, Volume 1, Special Issue of the Journal of the Geological Society of India,
DOI: 10.1007/978-81-322-1170-9_18,

Shirey 1999a, b; Richardson et al. 2001; Shirey and Richardson 2011). Diamond growth could occur during discrete growth episodes (Rudnick et al. 1993; Taylor et al. 1995), and dating diamonds is not an easy task. Diamond cannot be directly dated using radiometric methods, and the lack of inclusions in diamonds means that only infrared absorption data on the diamond-hosted nitrogen impurities can provide any age constraints (Evans and Qi 1982; Evans and Harris 1989; Boyd et al. 1994, 1995; Mendelssohn and Milledge 1995; Taylor et al. 1996a, b). The aggregation of nitrogen in diamond is sensitive to both temperature and time and could be used as an indication of the diamond residence time in the mantle (e.g. Evans and Harris 1989; Mendelssohn and Milledge 1995).

Silicate inclusion-bearing diamonds at Finsch (Appleyard et al. 2004) and Premier (Chinn et al. 2003) display complex internal growth patterns in cathodoluminescence and distinct infrared absorption characteristics (FTIR) within individual diamonds. These observations suggest that individual diamonds have experienced slight changes in temperature conditions during prolonged diamond formation or multiple diamond growth episodes over time. Complex diamond growth histories indicative of changes in a growth environment within the mantle have been previously stated from cathodoluminescence images, FTIR characteristics and multiple inclusion chemistry in single diamond (e.g. Bulanova 1995; Sobolev and Yefimova 1998; Taylor and Anand 2004; Taylor et al. 1996a, b, 2000; Spetsius and Taylor 2008). Distinct diamond events of growth, resorption and regrowth separated by billions of years have been suggested in Udachnaya diamonds based on Pb and Re–Os isotopes (Rudnick et al. 1993; Bulanova et al. 1998; Pearson et al. 1999b; Wiggers de Vries et al. 2008).

In order to evaluate the complexity of diamond genesis, we have modelled the infrared characteristics of 21 diamonds from Finsch (South Africa), 1 from Udachnaya (Siberia) and 18 from Premier (South Africa).

Geological Settings and Samples

The Finsch kimberlite is located 37 km east of Postmasburg and 160 km north-west of Kimberley, Cape Province, Republic of South Africa. The kimberlite is of Group II variety with an estimated Rb–Sr emplacement age of 118 Ma (Smith et al. 1985). The geology and petrology of the kimberlite have been described in Ruotsala (1975), Clement (1975) and Skinner et al. (1979). The inclusion suite of diamonds at Finsch is predominantly peridotitic (Harris and Gurney 1979). The genesis ages for the peridotitic-type (P) and eclogitic-type (E) diamonds are quite distinct, yielding a CHUR-based model age of 3.19 ± 0.05 Ga (Richardson et al. 1984) for the former and an isochron age of 1.58 ± 0.05 Ga for the latter (Richardson et al. 1990). Diamonds examined in this study all contained sulphide inclusions. All sulphide inclusions in the diamonds except F215 and F218 have high (>44 wt %) Fe, low-to-moderate (<13 wt %) Ni contents and so may be classified as E-type according to the sulphide Ni contents (Yefimova et al. 1983). Diamonds F215 and F218 are therefore classified as P-type which is consistent with a single purple P-type garnet inclusion recovered in the F215. Cathodoluminescence (CL) mapping reveals internal growth structures characterized by different $\delta^{13}C$ and N-abundances (Palot et al. 2013). However, core–rim relationships cannot be derived since the analyses were conducted on diamond fragments. Some diamond fragments exhibit complex growth pattern with non-regular octahedral growth patterns (Fig. 1). Appleyard et al. (2004) also identified CL distinct periods of growth within individual diamonds, resulting in both cubic and octahedral growth layers.

The Udachnaya kimberlite (Siberia) with an age of 350 Ma (Kinny et al. 1997) lies within the central Siberian platform (Sobolev and Nixon 1987). A single diamond examined in this study (diamond plate 3648) has been described in detail by Rudnick et al. (1993), Taylor et al. (1995) and Pearson et al. (1999b). The diamond central, cubo-octahedral zone contains a cluster of sulphide inclusions, a wustite inclusion and an Mg-rich olivine. The intermediate zone is octahedral, truncated by the rim zone indicative of a resorption event. The sulphide inclusions located in the rim zone are surrounded by cracks, one of which is re-healed. The high Ni and Os contents of the sulphide inclusions are consistent with the presence of olivine and therefore the P-type paragenesis of the diamond (Pearson et al. 1998).

The Premier kimberlite is located 30 km east–northeast of Pretoria in Republic of South Africa. The kimberlite is Precambrian in age (Allsopp et al. 1967; Barrett and Allsopp 1973). For a detailed review of its geology and petrology, see for example Scott and Skinner (1979). Samples examined here comprised one peridotitic (diamond AP28) and seventeen eclogitic silicate inclusion-bearing diamonds (Chinn et al. 2003). Most of diamonds exhibit octahedral zonations with indications of slight internal resorption (Chinn et al. 2003). E-type diamond AP28 is much more resorbed than the majority of other E-type diamonds at Premier and presents deformation lamellae features. Chinn et al. (2003) reported the complex diamond growth history of one E-type diamond AP33 studied in double-polished central plate (not analysed in this study). This sample comprises a well-defined core region characterized by high nitrogen aggregation state, which is surrounded by a low aggregation state rim overgrowth.

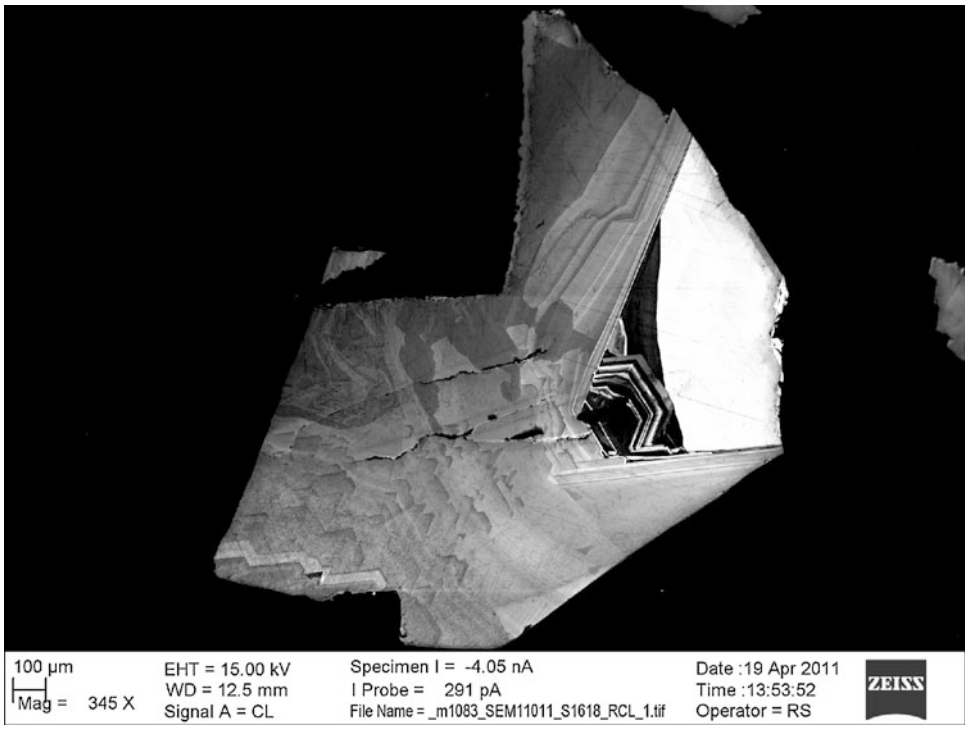

Fig. 1 Cathodoluminescence images of Finsch E-type diamond fragment F213-2 which exhibits non-regular octahedral growth patterns

Analytical Technique

Nitrogen abundances and nitrogen aggregation states, the latter measured as a percentage of nitrogen present in the fully aggregated B-defect, were determined in the De Beers Laboratory of Diamond Research at the University of Alberta, using a Thermo Nicolet Nexus 470 FT-IR spectrometer (bench) fitted with a continuum infrared microscope. Finsch diamond fragments were 1.5–4.5 mm in diameter and mainly were bounded by (111) cleavage planes. Spectra (650–4,000 cm^{-1}) were acquired in transmission mode for 200 s with a resolution of 4 cm^{-1} and an aperture size of 100 µm. Nitrogen concentrations and aggregation states were calculated after spectral decomposition using the Excel program CAXBD97, developed by David Fischer (the Diamond Trading Company, Maidenhead, UK). The absorption coefficients for the A and B centres at 1,282 cm^{-1} were 16.5 and 79.4 at.ppm/cm, respectively (Boyd et al. 1994, 1995). Detection limits and errors typically range from 5 to 20 ppm and about 10 %, respectively. The error of the aggregation state of nitrogen is estimated to be better than ±5 % (2σ).

Udachnaya sample 3648 and the Premier diamonds were diamond plates, polished mainly in (100) and (110) crystallographic directions. The Udachnaya diamond plate is approximately 7 mm long, and Premier plates range in weight between 60 and 200 mg. Data for 3648 were acquired using the equipment and techniques outlined by Mendelssohn and Milledge (1995). For the Premier samples, spectra were acquired with a Nicolet Magna 760 IR spectrometer, over the infrared range from 4,000 to 650 cm^{-1}. Data were processed using the same parameters and method described for the Finsch samples. The Premier data have been described briefly in abstract form by Chinn et al. (2003).

Results: Nitrogen Abundances and Aggregation States

Nitrogen abundances of Finsch samples were determined on 53 diamond fragments from 21 whole diamonds broken to release the inclusions. Overall, the nitrogen content in the studied diamonds ranges from 21 to 1,093 at.ppm (mean 569 ± 271 at.ppm, 1σ) (Table 1). Internal heterogeneity in N-abundance within single diamond ranges from 5 to 336 at.ppm (mean 141 ± 109 at.ppm, 1σ) (Figs. 2 and 3a). Since the analyses were conducted on diamond fragments, core–rim relationships generally cannot be derived. Overall nitrogen aggregation states (expressed as % of B-defects) vary from 0 to 83 % (mean 31 ± 21 %, 1σ) (Table 1). Internal variations of %B are from 2 to 60 % (mean 14 ± 14 %, 1σ) (Figs. 2 and 3a). Diamonds F203, F211, F213 and F215 display the largest variations in N-abundance and aggregation state (Figs. 2 and 3a).

Table 1 Finsch diamond measurements of nitrogen abundance and aggregation state by infrared spectroscopy

Sample	Inclusions	(N) (ppm)	(N) (at.ppm)	% B
F201-1	8 sulph. frag	n.a	n.a.	n.a
F201-2		570	489	6
F201-3		748	641	4
F202-1	15 sulph. frag	425	364	14
F202-2		413	354	8
F203-1	3 sulph. frag	751	644	57
F203-2	+ 1 whole sulph.	770	660	57
F203-3		898	770	56
F203-4		417	357	60
F203-5a		57	49	9
F203-5b		25	21	0
F203-6		225	193	51
F204-1	7 sulph. frag	976	837	36
F204-2		1275	1093	52
F205-1	11 sulph. frag	925	793	27
F205-2		722	619	31
F206-1	1 whole sulph.	767	657	31
F206-2		665	570	40
F206-3		732	627	29
F207-1	1 whole sulph	855	733	79
F207-2		1230	1054	83
F207-3		1223	1048	83
F208-1	1 whole sulph	1261	1081	30
F208-2		1273	1091	33
F208-3		435	373	23
F208-4		645	553	31
F209-1	9 sulph. frag	1160	994	38
F209-2		863	740	25
F210-1	7 sulph. frag	n.a	n.a.	n.a
F210-2		965	827	27
F211-1	19 sulph. frag	779	668	54
F211-2		869	745	31
F212-1	6 sulph. frag	425	364	44
F212-2	from 2 whole sulph	407	349	48
F212-3		526	451	56
F213-1	5 sulph. frag	544	466	58
F213-2		876	751	25
F213-3		620	531	52
F214-1	10 sulph. frag	697	597	28
F214-2	From 3 whole sulph.	679	582	30
F214-3		681	584	28
F214-4		868	744	32
F215-1	4 sulph. frag	359	308	59
F215-2	+ P-type garnet	273	234	41
F215-3		396	339	24
F216-1	5 sulph. frag	71	61	11
F216-2		26	22	2
F216-3		26	22	2
F217-1	19 sulph. frag	562	482	21
F217-2	+ 1 whole sulph.	319	273	19
F217-3		569	488	14
F218-1	3 sulph. frag	315	270	11
F218-2		257	220	2
F218-3		341	292	12
F219-1	16 sulph. frag	1217	1043	17
F219-2		1231	1055	13
F220-1	11 sulph. frag	710	609	23
F220-2		719	616	18
F221-1	2 sulph. frag	595	510	34
F221-2		589	505	23

Errors on nitrogen abundance and aggregation state are 15 % and ± 3 % (2σ), respectively. Abbreviations *sulph* sulphide, *frag* fragment

Nitrogen abundances of Udachnaya diamond 3648 range from 10 to 482 at.ppm (mean 194 ± 143 at.ppm, 1σ) (Table 2). Nitrogen content progressively decreases from the core to the rim. Nitrogen content in the inner core ranges from 482 to 311 at.ppm (mean 376 ± 44 at.ppm), in the outer core from 289 to 135 at.ppm (mean 230 ± 47 at.ppm, 1σ), in the intermediate zone from 113 to 37 at.ppm (mean 57 ± 27 at.ppm, 1σ) and in the rim from 94 to 10 at.ppm (mean 39 ± 25 at.ppm, 1σ) (Fig. 3b). Aggregation states vary from 14 to 86 % (mean of 31 ± 21 %, 1σ). Diamond 3648 also displays a decrease of %B from the core to the rim. The inner core varies from 86 to 69 % (mean 74 ± 4 %, 1σ), the outer core from 69 to 50 % (mean 62 ± 6 %, 1σ), the intermediate zone from 44 to 27 % (mean 35 ± 6 %, 1σ) and the rim from 44 to 14 % (mean 24 ± 8 %, 1σ) (Fig. 3b). The maximum variation in N-abundance and aggregation state between the inner core and the rim in diamond 3648 is 472 at.ppm and 72 %B, respectively (Fig. 2).

Overall, N-abundances in diamonds from Premier range from 21 to 802 at.ppm (mean 408 ± 166 at.ppm, 1σ) (Chinn et al. 2003, Fig. 3c). Internal variation in N-abundance within individual diamonds ranges from 93 to 654 at.ppm (mean of 320 ± 142 at.ppm, 1σ) (Fig. 2). Some diamonds exhibit spatial relationships in N-characteristics (Chinn et al. 2003). Nitrogen aggregation states vary from 2 to 65 % (mean 28 ± 11 %, 1σ) (Chinn et al. 2003, Fig. 3c). Internal variations of %B are from 7 to 62 % (mean of

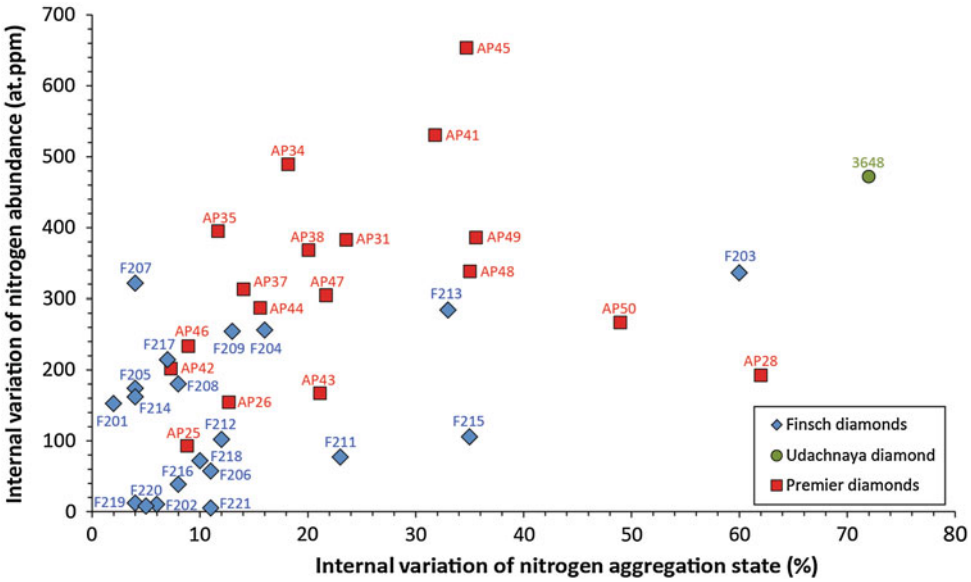

Fig. 2 Internal variation in nitrogen abundance (atomic.ppm) and aggregation state (% of B-defect) within individual diamonds from Premier (*square*), Udachnaya (*circle*) and Finsch (diamond). Internal variation represents the largest measured difference in N-abundance and %B for each diamond

24 ± 15 %, 1σ) (Fig. 2). Diamonds AP28, AP31, AP 41, AP45, AP49 and AP50 display the largest variations in N-abundance and %B (Figs. 2 and 3b, Table 3).

Discussion

Nitrogen Geothermometry

The most common atomic impurity in diamond is nitrogen (Kaiser and Bond 1959), and based on this element, diamonds have been classified as Type I, if nitrogen is present, and Type II, if it is absent (<20 ppm detection level). According to micro-FTIR studies of inclusion-bearing diamonds, 70 % is classified as Type I (Deines et al. 1989; Cartigny 2005; Stachel 2007; Stachel et al. 2009). The different nitrogen-bearing defects in diamonds are linked by a diffusion process. The initially single nitrogen atoms (i.e. the C-defect or diamond Type Ib) diffuse fairly rapidly over millions of years due to a low activation energy (Taylor et al. 1996a, b), to form pairs of nitrogen atoms (i.e. the A-defect or diamond Type IaA). Subsequently, the latter diffuses over billions of years, due to a higher activation energy (Evans and Qi 1982; Evans and Harris 1989), to form aggregates of nitrogen atoms tetrahedrally arranged around a vacancy (i.e. the B-defect or diamond Type IaB). The conversions both from Type Ib to Type IaA and then from Type IaA to Type IaB follow second-order kinetics. In the more important second nitrogen sequence, nitrogen abundance ([N] = [A-defect] + [B-defect]), the average residence time (t) and the storage temperature (T) are all linked by the following formula (Chrenko et al. 1977):

$$\frac{1}{[A-\text{defect}]}-\frac{1}{[N]}=\left(A\times\exp^{-\frac{Ea}{RT}}\right)\times t$$

N-abundance and A-defect are in atomic ppm of nitrogen, t is in seconds and T is in Kelvin, A and R are constants with A = 294,000 $\text{ppm}^{-1}\cdot\text{s}^{-1}$ and R = 8.317 $\text{J}\cdot\text{mol}^{-1}\cdot\text{K}^{-1}$, Ea = 675,510 $\text{J}\cdot\text{mol}^{-1}$ is the activation energy (Cooper 1990). Because mantle storage of diamonds is generally over hundreds of Ma, nitrogen aggregation depends chiefly on its time-integrated storage temperature. Nitrogen aggregation is therefore a valuable geothermometer (e.g. Evans and Harris 1989; Palot et al. 2009), which will be used in the next section in order to estimate mantle storage temperatures for the studied diamonds.

Multiple Growth Events for Finsch Sulphide Inclusion-Bearing Diamonds Inferred from Nitrogen Characteristics

In order to investigate the diamond growth histories, we have estimated their probable temperature ranges of formation. To do this calculation, we assume an average mantle residence time of ~1.4 Ga for the Finsch eclogitic sulphide inclusion-bearing diamonds (based on the genesis isochron age of 1.58 Ga for E-type silicate inclusions from Richardson et al. 1990, less than that of the eruption age of 118 Ma from Smith et al. 1985). The estimated mantle storage temperatures for the Finsch diamond fragments range from 1,068 to 1,174 °C with a mean of 1,128 ± 25 °C (1σ) (Fig. 3a). It is noticeable that changes in mantle residence time of the diamonds would affect the absolute storage temperature estimates, but do not alter our conclusions based on relative temperatures between

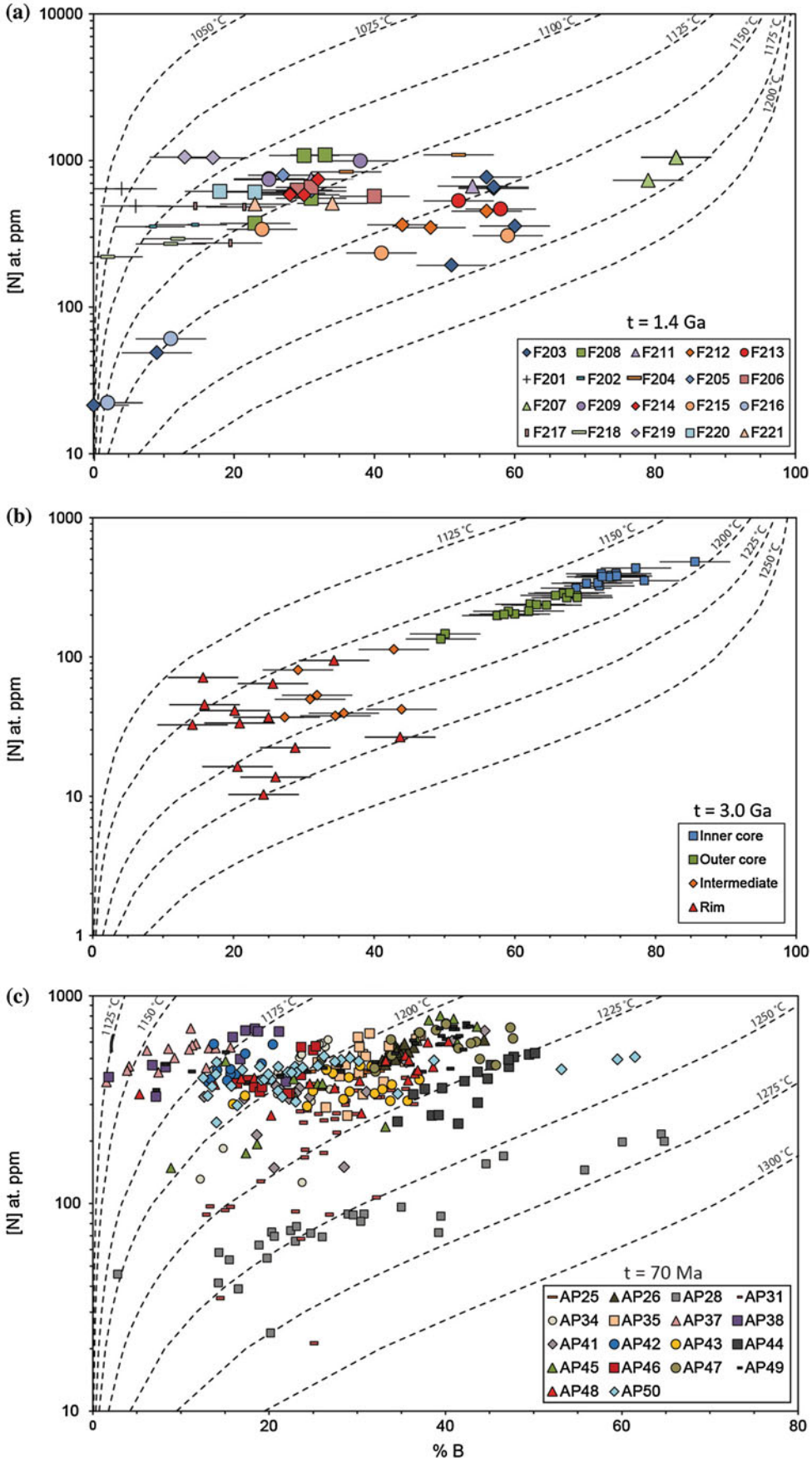

Fig. 3 Nitrogen abundance and aggregation state (%B) of diamonds from **a** Finsch, **b** Udachnaya and **c** Premier. Isotherms are calculated according to the second-order kinetic law for nitrogen diffusion (Chrenko et al. 1977) assuming an averaged mantle residence time of 1.4, 3.0 Ga and 70 Ma, respectively. Total errors of N-abundance and aggregation state are of 15 % and better than ±3 %, respectively. Errors bars are not represented for Premier diamonds for clarity

Table 2 Udachnaya diamond 3648 measurements of nitrogen abundance and aggregation state from core to rim by infrared spectroscopy

Sample	Approximate location	(N) (ppm)	(N) (at.ppm)	%B
B3648TEJ.1	Inner core	461	395	72
B3648TEK.1	Inner core	450	386	74
B3648TEL.1	Inner core	437	375	74
B3648TEW.1	Inner core	462	396	74
B3648TEX.1	Inner core	436	374	74
B3648TEY.1	Inner core	377	323	72
B3648TSJ.1	Inner core	397	340	72
B3648TSK.1	Inner core	444	381	75
B3648TSL.1	Inner core	394	338	70
B3648TSM.1	Inner core	363	311	69
B3648TEH.1	Inner core	412	353	78
B3648TEJ.1	Inner core	506	434	77
B3648TEK.1	Inner core	440	377	72
B3648TEL.1	Inner core	562	482	86
B3648TEF.1	Outer core	231	198	58
B3648TEG.1	Outer core	279	239	62
B3648TEH.1	Outer core	333	285	67
B3648TEM.1	Outer core	321	275	69
B3648TEN.1	Outer core	275	236	65
B3648TEP.1	Outer core	237	203	60
B3648TEZ.1	Outer core	310	266	67
B3648TSE.1	Outer core	171	147	50
B3648TSF.1	Outer core	248	213	59
B3648TSG.1	Outer core	322	276	66
B3648TSH.1	Outer core	337	289	68
B3648TSN.1	Outer core	276	237	63
B3648TSP.1	Outer core	235	201	59
83648TSQ.1	Outer core	157	135	50
B3648TEF.1	Outer core	249	213	62
B3648TEG.1	Outer core	311	267	69
B3648TEA.1	Intermediate	49	42	44
B3648TEB.1	Intermediate	46	39	36
B3648TEC.1	Intermediate	43	37	27
B3648TED.1	Intermediate	62	53	32
B3648TEE.1	Intermediate	94	81	29
B3648TEQ.1	Intermediate	132	113	43
B3648TSR.1	Intermediate	58	50	31
B3648TEA.1	Intermediate	44	38	35
B3648TER.1	Rim	75	64	26
B3648TES.1	Rim	43	37	25
B3648TET.1	Rim	16	14	26
B3648TEU.1	Rim	26	22	29
B3648TEV.1	Rim	110	94	34
B3648TSA.1	Rim	31	27	44
B3648TSB.1	Rim	12	10	24
B3648TSC.1	Rim	19	16	21
B3648TSD.1	Rim	48	41	20
B3648TSS.1	Rim			18
B3648TEB.1	Rim	39	33	21
B3648TEC.1	Rim	38	33	14
B3648TED.1	Rim	53	45	16
B3648TEE.1	Rim	83	71	16

Errors are reported in Table 1

different portions of diamond. Although Finsch diamonds are commonly thought to originate from a relatively homogenous carbon source (Deines et al. 1984), that conclusion was largely based on P-type diamond study. Heterogeneities in N-abundance and aggregation states in some Finsch E-type sulphide inclusion-bearing diamonds suggest that these samples experienced a relatively complex growth and mantle residence history as the data do not plot on a single isotherm (Fig. 3a). For example, diamonds F203, F211, F213, F215 and F218 show internal variations in their integrated mantle residence temperatures of up to ~50 °C (Fig. 3a). These variations reflect either slight changes in temperature conditions during prolonged diamond formation or distinct residence histories for different portions of the diamond, that is, multiple episodes of diamond growth extending over millions to billions of years (e.g. Appleyard et al. 2004; Taylor and Anand 2004). A steady increase in temperatures from the core to the rim is physically unacceptable, since the core must have experienced the same heating event. Therefore, unless these diamonds grew continuously over the course of millions of years while associated with a significant drop in ambient temperature, it is likely that multiple growth episodes occurred at different times. Assuming that the different portions in a single diamond that give the largest heterogeneity in N-abundance and aggregation (Fig. 2) represent distinct growth steps, we modelled the age differences of different portions within the single diamond using the equation of Chrenko et al. (1977) linking temperature, nitrogen abundance and average time residence. We assumed a maximum storage temperature of 1,174 °C based on maximum nitrogen temperature, consistent with the maximum inclusion-based temperature of 1,179 °C reported for E-type silicate-bearing Finsch diamonds (Appleyard et al. 2004). Uncertainties on nitrogen temperatures are of ±12 °C and are based on uncertainties of N-abundance and %B, leading to large uncertainties in time estimates. Our calculations indicate that the time between distinct growth

Table 3 Premier diamond measurements of nitrogen abundance and aggregation state by infrared spectroscopy

Sample	Paragenesis	(N) (at.ppm)	%B	Sample	Paragenesis	N (at.ppm)	%B
AP25	Eclogitic	436	32	AP42	Eclogitic	584	20
AP25	Eclogitic	438	31	AP42	Eclogitic	473	19
AP25	Eclogitic	449	32	AP42	Eclogitic	420	16
AP25	Eclogitic	429	32	AP42	Eclogitic	390	18
AP25	Eclogitic	413	30	AP42	Eclogitic	419	16
AP25	Eclogitic	401	29	AP42	Eclogitic	586	14
AP25	Eclogitic	413	29	AP42	Eclogitic	526	17
AP25	Eclogitic	416	28	AP42	Eclogitic	391	15
AP25	Eclogitic	410	28	AP42	Eclogitic	384	13
AP25	Eclogitic	406	28	AP42	Eclogitic	397	13
AP25	Eclogitic	356	26	AP42	Eclogitic	440	14
AP25	Eclogitic	359	27	AP42	Eclogitic	444	16
AP25	Eclogitic	362	26	AP43	Eclogitic	424	23
AP25	Eclogitic	377	25	AP43	Eclogitic	331	17
AP25	Eclogitic	425	27	AP43	Eclogitic	302	16
AP25	Eclogitic	432	25	AP43	Eclogitic	405	29
AP25	Eclogitic	440	24	AP43	Eclogitic	425	27
AP25	Eclogitic	448	24	AP43	Eclogitic	346	29
AP26	Eclogitic	461	32	AP43	Eclogitic	339	32
AP26	Eclogitic	469	33	AP43	Eclogitic	294	24
AP26	Eclogitic	517	35	AP43	Eclogitic	312	36
AP26	Eclogitic	554	35	AP43	Eclogitic	312	34
AP26	Eclogitic	560	35	AP43	Eclogitic	374	34
AP26	Eclogitic	536	34	AP43	Eclogitic	395	37
AP26	Eclogitic	566	36	AP43	Eclogitic	318	28
AP26	Eclogitic	615	44	AP43	Eclogitic	355	33
AP26	Eclogitic	538	36	AP43	Eclogitic	348	25
AP26	Eclogitic	522	35	AP43	Eclogitic	459	32
AP26	Eclogitic	495	34	AP43	Eclogitic	461	30
AP26	Eclogitic	487	33	AP43	Eclogitic	442	27
AP26	Eclogitic	489	33	AP44	Eclogitic	389	42
AP26	Eclogitic	503	33	AP44	Eclogitic	266	38
AP26	Eclogitic	557	34	AP44	Eclogitic	248	35
AP26	Eclogitic	575	34	AP44	Eclogitic	267	39
AP26	Eclogitic	588	35	AP44	Eclogitic	243	41
AP26	Eclogitic	567	34	AP44	Eclogitic	306	44
AP26	Eclogitic	538	34	AP44	Eclogitic	400	45
AP28	Peridotitic	170	47	AP44	Eclogitic	456	47
AP28	Peridotitic	155	45	AP44	Eclogitic	522	49
AP28	Peridotitic	73	20	AP44	Eclogitic	508	48
AP28	Peridotitic	46	3	AP44	Eclogitic	530	50
AP28	Peridotitic	58	14	AP44	Eclogitic	464	45
AP28	Peridotitic	74	22	AP44	Eclogitic	494	47
AP28	Peridotitic	77	23	AP44	Eclogitic	431	44

(continued)

Table 3 (continued)

Sample	Paragenesis	(N) (at.ppm)	%B	Sample	Paragenesis	N (at.ppm)	%B
AP28	Peridotitic	70	21	AP44	Eclogitic	360	40
AP28	Peridotitic	41	14	AP44	Eclogitic	336	36
AP28	Peridotitic	24	20	AP44	Eclogitic	357	38
AP28	Peridotitic	39	17	AP45	Eclogitic	485	15
AP28	Peridotitic	54	16	AP45	Eclogitic	398	23
AP28	Peridotitic	72	25	AP45	Eclogitic	326	23
AP28	Peridotitic	89	31	AP45	Eclogitic	175	17
AP28	Peridotitic	96	35	AP45	Eclogitic	193	19
AP28	Peridotitic	87	39	AP45	Eclogitic	148	9
AP28	Peridotitic	198	60	AP45	Eclogitic	234	33
AP28	Peridotitic	216	64	AP45	Eclogitic	596	41
AP28	Peridotitic	200	65	AP45	Eclogitic	712	44
AP28	Peridotitic	145	56	AP45	Eclogitic	775	41
AP28	Peridotitic	72	39	AP45	Eclogitic	765	38
AP28	Peridotitic	82	30	AP45	Eclogitic	802	39
AP28	Peridotitic	66	23	AP45	Eclogitic	609	37
AP28	Peridotitic	63	19	AP45	Eclogitic	378	26
AP28	Peridotitic	89	29	AP45	Eclogitic	378	26
AP28	Peridotitic	88	30	AP45	Eclogitic	515	29
AP28	Peridotitic	54	20	AP46	Eclogitic	393	18
AP28	Peridotitic	69	26	AP46	Eclogitic	380	16
AP31	Eclogitic	278	23	AP46	Eclogitic	363	18
AP31	Eclogitic	270	25	AP46	Eclogitic	345	19
AP31	Eclogitic	252	26	AP46	Eclogitic	365	19
AP31	Eclogitic	220	27	AP46	Eclogitic	340	22
AP31	Eclogitic	182	24	AP46	Eclogitic	339	22
AP31	Eclogitic	167	24	AP46	Eclogitic	416	24
AP31	Eclogitic	128	19	AP46	Eclogitic	549	25
AP31	Eclogitic	107	32	AP46	Eclogitic	568	24
AP31	Eclogitic	21	25	AP46	Eclogitic	572	25
AP31	Eclogitic	35	14	AP47	Eclogitic	497	26
AP31	Eclogitic	68	23	AP47	Eclogitic	616	34
AP31	Eclogitic	88	26	AP47	Eclogitic	666	37
AP31	Eclogitic	92	23	AP47	Eclogitic	737	40
AP31	Eclogitic	93	15	AP47	Eclogitic	731	40
AP31	Eclogitic	97	15	AP47	Eclogitic	685	39
AP31	Eclogitic	97	13	AP47	Eclogitic	517	34
AP31	Eclogitic	88	12	AP47	Eclogitic	432	32
AP31	Eclogitic	175	26	AP47	Eclogitic	450	32
AP31	Eclogitic	302	36	AP47	Eclogitic	560	41
AP31	Eclogitic	357	35	AP47	Eclogitic	602	43
AP31	Eclogitic	365	33	AP47	Eclogitic	592	43
AP31	Eclogitic	326	32	AP47	Eclogitic	704	47
AP31	Eclogitic	325	32	AP47	Eclogitic	624	48

(continued)

Table 3 (continued)

Sample	Paragenesis	(N) (at.ppm)	%B	Sample	Paragenesis	N (at.ppm)	%B
AP31	Eclogitic	404	35	AP47	Eclogitic	464	46
AP31	Eclogitic	352	33	AP47	Eclogitic	497	44
AP31	Eclogitic	270	29	AP48	Eclogitic	336	5
AP31	Eclogitic	256	27	AP48	Eclogitic	400	17
AP31	Eclogitic	300	28	AP48	Eclogitic	414	20
AP31	Eclogitic	351	30	AP48	Eclogitic	373	14
AP31	Eclogitic	314	28	AP48	Eclogitic	402	18
AP31	Eclogitic	272	27	AP48	Eclogitic	406	20
AP31	Eclogitic	246	23	AP48	Eclogitic	377	25
AP31	Eclogitic	281	24	AP48	Eclogitic	266	20
AP34	Eclogitic	394	19	AP48	Eclogitic	455	39
AP34	Eclogitic	423	23	AP48	Eclogitic	516	35
AP34	Eclogitic	455	23	AP48	Eclogitic	389	30
AP34	Eclogitic	505	23	AP48	Eclogitic	424	37
AP34	Eclogitic	568	26	AP48	Eclogitic	392	36
AP34	Eclogitic	592	26	AP48	Eclogitic	360	27
AP34	Eclogitic	615	27	AP48	Eclogitic	490	36
AP34	Eclogitic	587	26	AP48	Eclogitic	597	38
AP34	Eclogitic	523	24	AP48	Eclogitic	604	40
AP34	Eclogitic	522	24	AP48	Eclogitic	488	33
AP34	Eclogitic	557	30	AP48	Eclogitic	439	37
AP34	Eclogitic	355	27	AP48	Eclogitic	272	30
AP34	Eclogitic	337	21	AP49	Eclogitic	536	15
AP34	Eclogitic	428	21	AP49	Eclogitic	468	8
AP34	Eclogitic	311	25	AP49	Eclogitic	432	11
AP34	Eclogitic	126	24	AP49	Eclogitic	352	7
AP34	Eclogitic	131	12	AP49	Eclogitic	363	15
AP34	Eclogitic	184	15	AP49	Eclogitic	384	17
AP35	Eclogitic	479	26	AP49	Eclogitic	449	26
AP35	Eclogitic	524	31	AP49	Eclogitic	461	28
AP35	Eclogitic	511	31	AP49	Eclogitic	528	34
AP35	Eclogitic	426	30	AP49	Eclogitic	641	39
AP35	Eclogitic	336	31	AP49	Eclogitic	691	41
AP35	Eclogitic	482	35	AP49	Eclogitic	738	42
AP35	Eclogitic	644	37	AP49	Eclogitic	696	39
AP35	Eclogitic	647	37	AP49	Eclogitic	691	40
AP35	Eclogitic	619	37	AP49	Eclogitic	617	40
AP35	Eclogitic	573	34	AP49	Eclogitic	591	36
AP35	Eclogitic	385	33	AP49	Eclogitic	712	41
AP35	Eclogitic	265	29	AP49	Eclogitic	707	42
AP35	Eclogitic	291	26	AP49	Eclogitic	713	42
AP35	Eclogitic	411	28	AP49	Eclogitic	632	41
AP35	Eclogitic	467	29	AP49	Eclogitic	582	39
AP35	Eclogitic	468	28	AP49	Eclogitic	587	39

(continued)

Table 3 (continued)

Sample	Paragenesis	(N) (at.ppm)	%B	Sample	Paragenesis	N (at.ppm)	%B
AP35	Eclogitic	567	30	AP49	Eclogitic	610	36
AP35	Eclogitic	660	31	AP49	Eclogitic	641	41
AP35	Eclogitic	633	30	AP49	Eclogitic	552	42
AP37	Eclogitic	561	13	AP49	Eclogitic	445	40
AP37	Eclogitic	503	9	AP49	Eclogitic	431	37
AP37	Eclogitic	560	14	AP49	Eclogitic	465	36
AP37	Eclogitic	557	9	AP49	Eclogitic	479	32
AP37	Eclogitic	589	12	AP49	Eclogitic	480	32
AP37	Eclogitic	578	11	AP49	Eclogitic	437	28
AP37	Eclogitic	553	11	AP49	Eclogitic	430	28
AP37	Eclogitic	565	16	AP49	Eclogitic	413	21
AP37	Eclogitic	458	4	AP49	Eclogitic	429	24
AP37	Eclogitic	437	4	AP49	Eclogitic	407	21
AP37	Eclogitic	450	13	AP50	Eclogitic	457	19
AP37	Eclogitic	385	2	AP50	Eclogitic	430	22
AP37	Eclogitic	428	7	AP50	Eclogitic	397	20
AP37	Eclogitic	698	11	AP50	Eclogitic	393	19
AP37	Eclogitic	546	6	AP50	Eclogitic	396	20
AP38	Eclogitic	464	7	AP50	Eclogitic	396	19
AP38	Eclogitic	407	2	AP50	Eclogitic	420	20
AP38	Eclogitic	327	7	AP50	Eclogitic	402	13
AP38	Eclogitic	387	22	AP50	Eclogitic	440	17
AP38	Eclogitic	412	16	AP50	Eclogitic	513	26
AP38	Eclogitic	454	8	AP50	Eclogitic	456	23
AP38	Eclogitic	496	17	AP50	Eclogitic	467	26
AP38	Eclogitic	634	16	AP50	Eclogitic	492	28
AP38	Eclogitic	681	17	AP50	Eclogitic	483	27
AP38	Eclogitic	696	18	AP50	Eclogitic	503	29
AP38	Eclogitic	675	19	AP50	Eclogitic	485	30
AP38	Eclogitic	674	21	AP50	Eclogitic	489	39
AP41	Eclogitic	326	13	AP50	Eclogitic	443	53
AP41	Eclogitic	320	17	AP50	Eclogitic	495	60
AP41	Eclogitic	368	21	AP50	Eclogitic	509	62
AP41	Eclogitic	353	21	AP50	Eclogitic	338	35
AP41	Eclogitic	333	23	AP50	Eclogitic	309	23
AP41	Eclogitic	360	23	AP50	Eclogitic	349	21
AP41	Eclogitic	341	23	AP50	Eclogitic	428	23
AP41	Eclogitic	319	22	AP50	Eclogitic	428	23
AP41	Eclogitic	326	25	AP50	Eclogitic	461	26
AP41	Eclogitic	480	36	AP50	Eclogitic	452	24
AP41	Eclogitic	679	44	AP50	Eclogitic	456	21
AP41	Eclogitic	607	41	AP50	Eclogitic	368	16
AP41	Eclogitic	345	31	AP50	Eclogitic	326	22
AP41	Eclogitic	150	28	AP50	Eclogitic	246	14

(continued)

Table 3 (continued)

Sample	Paragenesis	(N) (at.ppm)	%B	Sample	Paragenesis	N (at.ppm)	%B
AP41	Eclogitic	148	21	AP50	Eclogitic	297	16
AP41	Eclogitic	214	19	AP50	Eclogitic	330	13
				AP50	Eclogitic	366	14
				AP50	Eclogitic	420	14
				AP50	Eclogitic	479	14

Errors are reported in Table 1

steps within individual diamonds varies from minimum estimates (mantle residence at 1,174 °C) of $\sim 3^{+88}_{-3}$ Ma (diamond F208) to 942 ± 368 Ma (diamond F215), to maximum estimates (residence at 1,000–1,140 °C at 4.5 Ga) that are equivalent to the age of the Earth (Fig. 4a). These calculations may be underestimated because the random orientation of fragments may be mixtures of zones with distinct FTIR characteristics. Because of the large uncertainties for some diamonds (F204, F205, F207, F208, F209, F212, F214, F219 and F220, Table 4), it cannot be ruled out that these samples may have experienced a single growth event at relatively constant temperature. The majority of our calculations are, however, compatible with multiple growth events during the formation of sulphide inclusion-bearing diamonds at Finsch. This implies that isochron ages may be flawed as there appears to be no single formation age for a single diamond. This is consistent with distinct carbon isotopic compositions and nitrogen contents observed across some of these diamonds (Palot et al. 2013).

Multiple Growth Events for Udachnaya Peridotitic Sulphide Inclusion-Bearing Diamond Inferred from Nitrogen Characteristics

We assume an average mantle residence time of ~3.0 Ga for the Udachnaya diamond 3648 (based on the model age of 3.1–3.5 Ga on sulphide inclusions in this diamond by Pearson et al. 1999b). The age of inclusions is significantly older than that of the eruption age of 361 Ma (Kinny et al. 1997). The estimated mantle storage temperatures range from 1,137 to 1,200 °C with a mean of 1,166 ± 12 °C (1σ) (Fig. 3b), which are within the range of inclusion-based temperatures of Udachnaya diamonds (e.g. Griffin et al. 1993). The inner and outer cores display a constant estimated storage temperature of 1,163 ± 3 °C (1σ) with data plotting close to the theoretical isotherms at constant time (Fig. 3b). In contrast, the intermediate and rim zones display more scattered time-averaged residence temperatures, with a slightly higher mean of 1,170 ± 17 °C (1σ) (Fig. 3b). A steady increase in integrated temperature from the core to the rim within mantle diamonds is physically implausible, since the former and the latter must have experienced the same temperature during any heating event, and diamonds conduct heat very efficiently. We therefore explore the possibility of multiple growth episodes at different times suggested by Rudnick et al. (1993) based on large variations in Pb isotopic compositions of sulphides included in this diamond and by Bulanova et al. (1996) and Pearson et al. (1999b) based on enriched Os, Re, Pb and Zn and more radiogenic Os and Pb isotopes in one sulphide inclusion in the rim of diamond 3648. Calculations indicate that the maximum relative time between the core and the rim varies from a minimum estimate (mantle residence at 1,200 °C) of ~2,387 ± 931 Ma to maximum estimate (residence at 1,186 °C) that is equivalent to the age of the Earth (Fig. 4b). The minimum estimate equals the estimate of 2 Ga as the age difference between different growth zones of this diamond determined by Pb-isotope analysis of sulphide inclusions by Rudnick et al. (1993).

Multiple Growth Events for Premier Silicate Inclusion-Bearing Diamonds Inferred from Nitrogen Characteristics

Eclogitic silicate inclusion-bearing diamonds at Premier display ages from 1,150 ± 60 to 1,254 Ma (Richardson 1986; Burgess et al. 1989; Phillips et al. 1989) compared to a pipe eruption age of 1,180 ± 30 Ma (Allsopp et al. 1989). We assume a maximum average mantle residence time of ~70 Ma for these diamonds. The estimated mantle storage temperatures range from 1,127 to 1,286 °C with a mean of 1,209 ± 23 °C (1σ) (Fig. 3c) and are slightly lower than estimates from inclusions in Premier diamonds (between 1,199 and 1,363 °C, Gurney et al. 1985). The large variations in N-abundance and aggregation states in some Premier diamonds suggest that these samples also have experienced complex growth histories. Variation in time-integrated storage temperature within individual diamonds ranges from 10 °C (diamond AP26) to 79 °C (diamond AP28) (Fig. 3c). These variations, which are similar to Finsch and Udachnaya diamonds, are interpreted as reflecting multiple episodes of diamond growth separated in time, rather than steady increases or decreases in storage temperature. Calculations indicate that the maximum time between distinct growth steps varies from minimum estimates (mantle residence at 1,286 °C) of 1.5 ± 0.5 Ma (diamond AP37) to 76 ± 23 Ma (diamond AP31), to

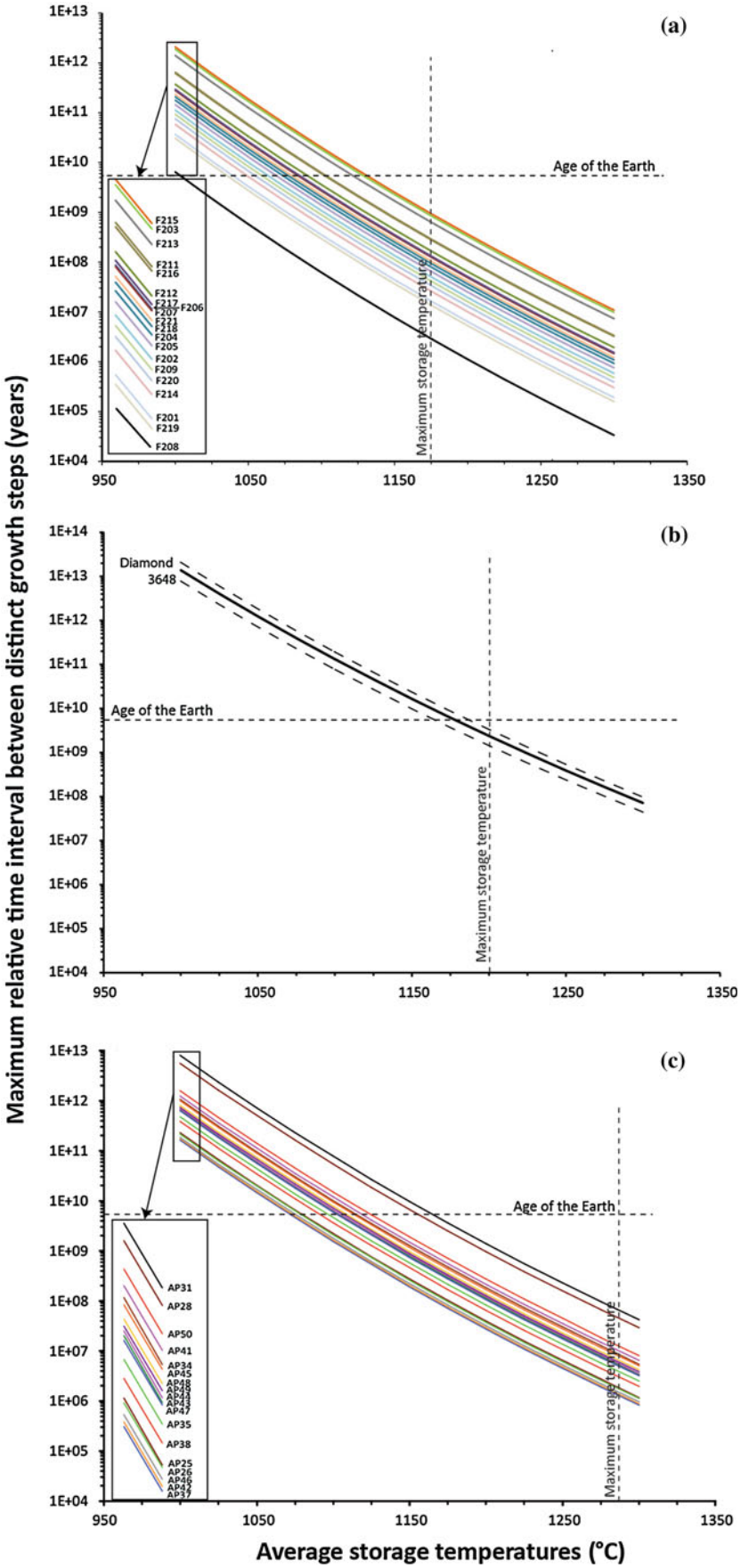

Fig. 4 Maximum relative times between distinct growth steps against averaged storage temperatures within individual diamonds from **a** Finsch, **b** Udachnaya and **c** Premier. The maximum averaged storage temperature for a given locality is based on the highest nitrogen (and inclusion)-based temperature estimate reported for each population. The age of the Earth is reported as the upper limit for time difference between distinct diamond portions. Errors bars (*dotted lines*) are only reported for Udachnaya diamond for clarity

Table 4 Relative errors (± %, 2σ) on temperature estimates for Finsch, Udachnaya and Premier diamonds at temperatures from 1,000 to 1,300 °C (50 °C increments)

Samples/Temperature	1,000 °C	1,050 °C	1,100 °C	1,150 °C	1,200 °C	1,250 °C	1,300 °C
F201	78.6	75.5	72.6	69.7	66.9	64.2	61.6
F202	89.6	86.1	82.7	79.4	76.2	73.2	70.2
F203	60.5	58.1	55.8	53.6	51.4	49.3	38.3
F204	132.9	127.7	122.6	117.7	113.0	108.5	104.1
F205	117.6	113.0	108.6	104.2	100.0	96.0	92.2
F206	91.3	87.7	84.3	80.9	77.6	74.5	72.4
F207	486.9	467.9	449.4	431.4	414.1	397.5	381.5
F208	3501.5	3364.7	3231.5	3102.4	2977.9	2858.1	2743.2
F209	162.9	156.5	150.3	144.3	138.5	133.0	127.6
F211	56.9	54.7	52.5	50.4	48.4	46.5	44.6
F212	188.7	181.3	174.1	167.2	160.5	154.0	142.0
F213	42.1	40.4	38.8	37.3	35.8	34.3	33.0
F214	330.6	317.7	305.1	292.9	281.2	269.9	262.2
F215	45.0	43.3	41.6	39.9	38.3	36.8	41.0
F216	70.7	67.9	65.2	62.6	60.1	57.7	55.4
F217	62.1	59.7	57.3	55.0	52.8	50.7	53.9
F218	45.0	43.2	41.5	39.9	38.3	36.7	34.6
F219	156.5	150.4	144.4	138.6	133.1	127.7	122.6
F220	159.3	153.1	147.0	141.2	135.5	130.1	124.8
F221	99.0	95.1	91.3	87.7	84.2	80.8	77.5
3648	22.9	22.0	21.2	20.3	19.5	18.7	18.0
AP25	112.4	108.0	103.8	99.6	95.6	91.8	88.1
AP26	144.6	139.0	133.5	128.1	123.0	118.1	113.3
AP28	37.7	36.2	34.8	33.4	32.1	30.8	29.5
AP31	38.1	36.6	35.2	33.8	32.4	31.1	29.9
AP34	47.8	45.9	44.1	42.3	40.6	39.0	37.4
AP35	69.5	66.8	64.1	61.6	59.1	56.7	54.4
AP37	40.8	39.2	37.6	36.1	34.7	33.3	32.0
AP38	37.8	36.3	34.9	33.5	32.2	30.9	29.6
AP41	43.0	41.4	39.7	38.1	36.6	35.1	33.7
AP42	73.9	71.0	68.2	65.5	62.8	60.3	57.9
AP43	58.0	55.7	53.5	51.4	49.3	47.3	45.4
AP44	97.6	93.8	90.1	86.5	83.0	79.7	76.5
AP45	43.4	41.7	40.0	38.4	36.9	35.4	34.0
AP46	105.8	101.6	97.6	93.7	90.0	86.3	82.9
AP47	62.2	59.7	57.4	55.1	52.9	50.7	48.7
AP48	39.7	38.1	36.6	35.1	33.7	32.4	31.1
AP49	40.6	39.0	37.4	35.9	34.5	33.1	31.8
AP50	39.9	38.4	36.9	35.4	34.0	32.6	31.3

maximum estimates (residence at 1,076–1,170 °C) that are equivalent to the age of the Earth (Fig. 4c). Marked variation in FTIR data suggests distinct and multiple growth episodes for E-type diamonds at Premier with ages minimal 1 Ma apart, in agreement with some conclusions of Chinn et al. (2003). A single diamond growth event cannot be ruled out for diamonds AP25, AP26 and AP46 due to large uncertainties (Table 4).

Overall, this study therefore suggests multiple episodes of diamond growth based on distinct infrared spectroscopy characteristics within individual macro-diamonds from different localities and parageneses. Similar evidence was found previously for eclogitic diamonds from Siberian kimberlites (Bulanova et al. 1998 and 2012) and by Wiggers de Vries et al. (2008, 2011) in a detailed study of sulphide-bearing diamond plates from Udachnaya, Mir and Mwadui kimberlites. The study by Wiggers de Vries et al. (2008) also revealed complex Re–Os isotope systematics in sulphides derived from different diamond growth zones, clearly indicating the complexity present in single diamond. FTIR study is therefore a valuable diagnostic tool in characterizing samples for radiometric dating. In addition, the technique is an excellent complement to classical CL images in selecting diamonds for in situ carbon isotopic profiles, allowing the ability to determine the likelihood of multiple growth events. Measurements for such work are best taken in situ on polished diamond plates, as for the Udachnaya and Premier diamonds, to preserve the relationships between the data points, using the CL image as a map of the growth history. In this way, any changes in crystal growth or periods of resorption can be integrated with the data measurements for interpretation.

Conclusions

The examination of 21 sulphide inclusion-bearing diamonds from Finsch, 1 sulphide inclusion-bearing diamond from Udachnaya and 18 silicate inclusion-bearing diamonds from Premier revealed distinct N-abundances and aggregation states of nitrogen within individual samples. These variations more likely reflect multiple growth episodes of diamond at different times rather than steady changes in temperature conditions during prolonged diamond formation. Modelling of these heterogeneities indicates that some diamonds have experienced distinct growth episodes over extended time periods, implying that great care is needed in the evaluation of isochron and model ages in radiometric dating studies, as there may be multiple phases of diamond growth in single diamond.

The diamonds investigated in this study were derived from different localities and parageneses, suggesting that such complex growth histories are not rare. Infrared characteristics are a critical tool for constraining diamond growth histories and for selecting diamonds for dating.

Acknowledgments The Finsch diamond samples used in this study were gifted to JWH by the Diamond Trading Company, a member of the DeBeers Group of Companies. The authors sincerely thank DeBeers for this material. The Udachnaya diamond plate was generously provided by the Diamond and Precious Metal Geology Institute, Siberian Branch, Russian Academy of Sciences. The Premier diamonds were made available for study by De Beers. We thank Judith Milledge for her FTIR measurements. The study was funded by a CERC award to D.G. Pearson. The authors express their appreciation to L.A. Taylor and D. Wiggers de Vries for their reviews, which has resulted in improvement to the manuscript and helped improve the ideas presented here.

References

Allsopp HL, Bristow JW, Smith CB, Brown R, Gleadow AJ, Kramers JD, Garvie O (1989) A summary of radiometric dating methods applicable to kimberlites and related rocks. In: Ross JL (ed) Kimberlite and related rocks: their composition, occurrence, origin and emplacement. Blackwell, Oxford, p 349

Allsopp HL, Burger AJ, van Zyl C (1967) A minimum age for the Premier kimberlite pipe yielded by Rb-Sr measurements with related galena isotopic data. Earth Planet Sci Lett 3:161–166

Appleyard CM, Viljoen KS, Dobbe R (2004) A study of eclogitic diamonds and their inclusions from the Finsch kimberlite pipe, South Africa. Lithos 77:317–332

Barrett DR, Alsopp HL (1973) Rubidium-strontium age determinations on South African kimberlite pipes. Extended abstract 1st international kimberlite conference, Cape Town, pp 23–25

Boyd SR, Kiflawi I, Woods GS (1994) The relationship between infrared absorption and A-defect concentration in diamond. Phil Mag B69:1149–1153

Boyd SR, Kiflawi I, Woods GS (1995) Infrared absorption by the B nitrogen aggregate in diamond. Phil Mag 72:351–361

Bulanova GP (1995) The formation of diamond. J Geochem Explor 53:1–23

Bulanova GP, Griffin WL, Ryan CG, Shestakova OY, Barnes S-J (1996) Trace elements in sulphide inclusions from Yakutian diamonds. Contrib Miner Petrol 124:111–125

Bulanova GP, Shelkov D, Milledge HJ, Hauri EH, Smith BC, Chris B (1998) Nature of eclogitic diamonds from Yakutian kimberlites: evidence from isotopic composition and chemistry of inclusions. In: Proceedings of 7th international kimberlite conference, vol 1. Red Roof Design, Cape Town, pp 57–65

Bulanova GP, Wiggers de Vries DF, Beard A, Pearson DG, Mikhail S, Smelov AP, Davies GR (2012). Two-stage origin of eclogitic diamonds recorded by a single crystal from Mir pipe (Yakutia). 10th international kimberlite conference extended abstract no. 10IKC-220

Burgess R, Turner G, Laurenzi M, Harris JW (1989) $^{40}Ar/^{39}Ar$ laser probe dating of individual clinopyroxène inclusions in Premier eclogitic diamonds. Earth Planet Sci Lett 94:22–28

Cartigny P (2005) Stables isotopes and the origin of diamond. Elements 1:79–84

Chinn I, Pienaar C, Kelly C (2003) Diamond growth histories at premier mine. Extended abstract 8 h international kimberlite conference victoria (British Columbia), pp 1–4

Chrenko RM, Tuft RE, Strong HM (1977) Transformation of the state of nitrogen in diamond. Nature 270:141–144

Clement CR (1975) The emplacement of some diatreme-facies kimberlite. In: Ahrens LH, Dawson JB, Duncan AR, Erlank AJ (eds) Physics and chemistry of the earth, vol 9. Pergamon Press, New York, pp 51–60

Cooper GI (1990) Infrared spectroscopy of diamond in relation to mantle processes. Ph.D. thesis, University of London

Deines P, Gurney JJ, Harris JW (1984) Associated chemical and carbon isotopic composition variations in diamonds from Finsch and Premier kimberlite, South Africa. Geochimica and Cosmochimica Acta 48:325–342

Deines P, Harris JW, Spear PM (1989) Nitrogen and ^{13}C content of Finsch and Premier diamonds and their implications. Geochimica and Cosmochimica Acta 53:1367–1378

Evans T, Harris JW (1989) Nitrogen aggregation, inclusion equilibration temperatures and the age of diamonds. In: Ross N (ed) Kimberlites and related rocks, vol 2. Geological Society Special Publication No. 14, pp 1001–1006

Evans T, Qi Z (1982) The kinetics of the aggregation of nitrogen atoms in diamond. Proceedings of the Royal Society of London A381, pp 159–178

Griffin WL, Sobolev NV, Ryan CG, Pokhilenko NP, Win TT, Yefimova ES (1993) Trace elements in garnets and chromites: diamond formation in the Siberian lithosphere. Lithos 29:235–256

Gurney JJ, Harris JW, Rickard RS, Moore RO (1985) Inclusions in premier mine diamonds. Trans Geol Soc S Afr 88:301–310

Harris JW, Gurney JJ (1979) Inclusions in diamond. In: Field JE (ed) Properties of diamond. Academic Press, London, pp 555–594

Kaiser W, Bond WL (1959) Nitrogen—a major impurity in common type I diamond. Phys Rev 115:857–863

Kinny PD, Griffin BJ, Heaman LM, Brakhfogel FF, Spetsius ZV (1997) SHRIMP U/Pb ages of perovskite and zircon from Yakutian kimberlites. Russ Geol Geophys 38:97–105

Mendelssohn M, Milledge HJ (1995) Geologically significant information from routine analysis of the mid-infrared spectra of diamonds. Int Geol Rev 37:95–110

Palot M, Cartigny P, Viljoen KS (2009) Diamond origin and genesis: A C and N stable isotope study on diamonds from a single eclogitic xenolith (Kaalvallei, South Africa). Lithos 112S:758–766

Palot M, Pearson DG, Stern T, Stachel T, Harris JW (2013) Multiple growth events, processes and fluid sources involved in the growth of sulphide-bearing diamonds from Finsch mine, RSA: a micro-analytical study. Geochim Cosmochim Acta 106:51–70

Pearson DG, Shirey SB (1999a) Isotopic dating of diamonds. In: Lambert DD, Ruiz J (eds) Application of radiogenic isotopes to ore deposit research and exploration, vol 12. Society of Economic Geologists, Boulder, pp 143–172

Pearson DG, Shirey SB, Bulanova GP, Carlson RW, Milledge HJ (1999b) Re-Os isotope measurements of single sulfide inclusions in a Siberian diamond and its nitrogen aggregation systematics. Geochim Cosmochim Acta 63:703–711

Pearson DG, Shirey SB, Harris JW, Carlson RW (1998) Sulfide inclusions in diamonds from the Koffiefontein kimberlite, S. Africa: constraints on diamond ages and mantle Re-Os systematics. Earth Planet Sci Lett 160:311–326

Phillips D, Onstott TC, Harris JW (1989) $^{40}Ar/^{39}Ar$ laser-probe dating of diamond inclusions from Premier kimberlite. Nature 340:460–462

Richardson SH (1986) Latter-day origin of diamonds of eclogitic paragenesis. Nature 322:623–626

Richardson SH, Erlank AJ, Harris JW, Hart SR (1990) Eclogitic diamonds of Proterozoic age from cretaceous kimberlites. Nature 346:54–56

Richardson SH, Gurney JJ, Erlank AJ, Harris JW (1984) Origin of diamonds in old enriched mantle. Nature 310:198–202

Richardson SH, Shirey SB, Harris JW, Carlson RW (2001) Archean subduction recorded by Re-Os isotopes in eclogitic sulfide inclusions in Kimberley diamonds. Earth Planet Sci Lett 191:257–266

Rudnick RL, Eldridge CS, Bulanova GP (1993) Diamond growth history from in situ measurement of Pb and S isotopic compositions of sulfide inclusions. Geology 21:13–16

Ruotsala AP (1975) Alteration of the Finsch kimberlite pipe, South Africa. Econ Geol 700:582–590

Scott BH, Skinner EMW (1979) The premier kimberlite pipe, Transvaal, South Africa. Extended abstract kimberlite symposium II

Shirey SB, Harris JW, Richardson SH, Fouch MJ, James DE, Cartigny P, Deines P, Viljoen SK (2002) Diamond genesis, seismic structure, and evolution of the Kaapvaal-Zimbabwe craton. Science 297:1683–1686

Shirey SB, Richardson SH (2011) Start of the Wilson cycle at 3 Ga shown by diamonds from subcontinental mantle. Science 333:434–436

Skinner EM, Clement CR (1979) Mineralogical classification of southern African kimberlites. In: Boyd FR, Meyer HOA (eds) Kimberlites, diatremes and diamonds: their geology, petrology, and geochemistry. Proceedings of the 2nd international kimberlite conference, vol 1. American Geophysical Union, pp 129–139

Smith CB, Allsopp HL, Kramers JD, Hutchinson G, Roddick JC (1985) Emplacement ages of Jurassic—cretaceous South African kimberlites by the Rb–Sr method on phlogopite and whole rock samples. Trans Geol Soc S Afr 88:249–266

Sobolev NV, Nixon PH (1987) Xenoliths from the USSR and Mongolia: a selective and brief review. In: Nixon PH (ed) Mantle xenoliths. Wiley, Chichester, pp 159–166

Sobolev NV, Yefimova ES (1998) The variation of chromite inclusions composition as indicator of zonation of diamonds. Dokladi Russian Akademii nauk 358(5):649–652

Spetsius ZV, Taylor LA (2008) Diamonds of Siberia photographic evidence for their origin. Tranquility Base Press, Lenoir City

Stachel T (2007) Diamond. Mineral Assoc Can Short Course Ser 37:1–22

Stachel T, Brey GP, Harris JW (2005) Inclusions in sublithospheric diamonds: glimpses of deep Earth. Elements 1:73–78

Stachel T, Harris JW, Muehlenbachs K (2009) Sources of carbon in inclusion bearing diamonds. Lithos 112S:625–637

Taylor LA, Anand M (2004) Diamonds: time capsules from the Siberian Mantle. Chem Erde 64:1–74

Taylor LA, Keller RA, Snyder GA, Wang W, Carlson WD, Hauri E, Kim KR, Sobolev NV, Bezborodov SM (2000) Diamonds and their mineral inclusions, what they tell us: a detailed "pull-apart" of a diamondiferous eclogite. Int Geol Rev 42:959–983

Taylor LA, Snyder GA, Crozaz G, Sobolev VN, Yefimova ES, Sobolev NV (1996a) Eclogitic inclusions in diamonds: evidence of complex mantle processes over time. Earth Planet Earth Sci Lett 142:535–551

Taylor WR, Bulanova GP, Milledge HJ (1995) Quantitative nitrogen aggregation study of some Yakutian diamonds: constraints on the growth, thermal and deformation history of peridotitic and eclogitic diamonds. Extended abstract 6th international kimberlite conference, Novosibirsk, pp 608–610

Taylor WR, Canil D, Milledge HJ (1996b) Kinetics of Ib to IaA nitrogen aggregation in diamond. Geochimica and Cosmochimica Acta 60:4725–4733

Wiggers de Vries DF, Harris JW, Pearson GP, Davis GR (2011) Re-Os isotope constraints on the ages of diamonds from Mwadui, Tanzania. Extended abstracts 10th international kimberlite conference, Bangalore 10IKC-203

Wiggers de Vries DF, Pearson DG, Bulanova GP, Pavlushin AD, Molotkov AE, Davies GR (2008). Comprehensive petrological and geochemical study of Yakutian diamonds focussing on Re-Os dating of multiple sulphides in single diamonds. Extended abstracts 9th international kimberlite conference, Frankfurt, p A309

Yefimova ES, Sobolev NV, Pospelova LN (1983) Sulfide inclusions in diamond and specific features of their paragenesis. Zapiski Vseoyuznogo Mineralogicheskogo Obshcestva 112:300–310